

Nuclear magnetic resonance on oriented $^{106}\text{Ag}^m$ in Fe and Ni

R. Eder, E. Hagn, and E. Zech

Physik-Department, Technische Universität München, D-8046 Garching, Federal Republic of Germany

(Received 13 March 1984)

The magnetic hyperfine splitting frequencies $\nu_m = |g\mu_N B_{\text{HF}}/h|$ of $^{106}\text{Ag}^m$ ($I^\pi=6^+$; $T_{1/2}=8.5$ d) as a dilute impurity in Fe and Ni have been measured with nuclear magnetic resonance on oriented nuclei at temperatures of ~ 10 mK as 210.57(3) MHz and 50.76(4) MHz, respectively. With the magnetic hyperfine field known from $^{110}\text{Ag}^m\text{Fe}$ to be $B_{\text{HF}}(\text{AgFe})=-446.9(5)$ kG, the magnetic moment of $^{106}\text{Ag}^m$ is derived as $(+)3.709(4)\mu_N$. The magnetic hyperfine field of Ag in Ni is deduced to be $-107.7(2)$ kG, which is in contradiction to the value in the literature. From the differential resonance displacements of γ transitions with different multipolarities, an upper limit for the electric quadrupole splitting of $^{106}\text{Ag}^m\text{Fe}$ is estimated. In addition, multipole mixing ratios for a series of transitions in ^{106}Pd were determined. The spin of the 2366 keV level of ^{106}Pd is determined to be $I=5$.

I. INTRODUCTION

In the even- A Ag isotopes isomeric states with $I^\pi=6^+$ appear at rather low excitation energies:¹ ^{106}Ag : $E=87.9$ keV, $T_{1/2}=8.5$ d; ^{108}Ag : $E=109.5$ keV, $T_{1/2}=127$ yr; ^{110}Ag : $E=117.7$ keV, $T_{1/2}=252$ d. The nuclear moments of the long-lived isotopes $^{108,110}\text{Ag}^m$ are known from optical hyperfine spectroscopy.² The magnetic moments of these states, $\mu(^{108}\text{Ag}^m)=3.580(20)\mu_N$ and $\mu(^{110}\text{Ag}^m)=3.607(4)\mu_N$ (Ref. 2, recalculated according to Ref. 1 with the diamagnetic shielding of Ref. 3), suggest the 6^+ state arising from the stretched coupling of $(\pi g_{9/2})_{7/2+}^{-3}$ and $(\nu d_{5/2})_{5/2+}^{-1}$ shell model states.^{4,2} The analogous state in ^{106}Ag has been the subject of two nuclear orientation (NO) studies^{5,6} utilizing the large hyperfine field acting on Ag as dilute impurity in iron.⁷ However, the solubility of Ag in Fe is known to be limited to $\leq 10^{-3}$,⁸ which may complicate the preparation of homogeneously diluted alloys necessary for the correct interpretation of NO experiments. Schoeters *et al.*⁵ prepared an alloy by quenching from 1200°C to room temperature in about 30 s. They derived a magnetic moment of $2.8(2)\mu_N$, which is considerably smaller than the magnetic moments of $^{108,110}\text{Ag}^m$. Haroutunian *et al.*⁶ performed a similar experiment on a quenched alloy containing activities of $^{106}\text{Ag}^m$ and $^{110}\text{Ag}^m$. By the simultaneous measurement of the γ anisotropies of analogous transitions from $^{110}\text{Ag}^m\text{Fe}$, the unknown fraction of Ag nuclei being subject to the full undisturbed hyperfine field cancels out to first approximation as the decay properties of $^{110}\text{Ag}^m$ and the hyperfine splitting of $^{110}\text{Ag}^m\text{Fe}$ are known with good accuracy. Their result for the magnetic moment, $\mu(^{106}\text{Ag}^m)=3.71(15)\mu_N$, was in better agreement with the expectation. In view of these facts, a more precise measurement was desirable. The nuclear magnetic resonance on oriented nuclei (NMR-ON) technique⁹ is well suited for the precise determination of hyperfine splitting frequencies of radioactive nuclei as dilute impurities in ferromagnetic metals (Fe, Co, and Ni). As the γ anisotropy serves only as the detector for NMR, its absolute value in-

fluences only the resonance amplitude, which means that the method is nearly independent of metallurgic properties such as the solubility, as long as the fraction of impurity nuclei on regular lattice sites is so large that the resonant destruction can be observed with statistical significance.

NMR-ON experiments on $^{110}\text{Ag}^m$ in Fe and Ni were first reported by Fox *et al.*¹⁰ Using sources prepared by diffusion, the zero-field hyperfine splittings in Fe and Ni were determined to be 204.8(2) and 56.0(2) MHz, respectively. Recently, Rüter *et al.*¹¹ performed NMR-ON measurements on the same systems, the samples being prepared by mass-separator implantations, with results of 204.78(1) and 49.40(4) MHz. While the resonance frequencies for Fe agree well, there is a large discrepancy for Ni. Thus a clarifying experiment with another isotope was desirable from this point of view, too.

Here we report on NMR-ON measurements on $^{106}\text{Ag}^m$ in Fe and Ni. For the sample preparation the recoil-implantation technique was applied. From these experiments a precise value for the magnetic moment of $^{106}\text{Ag}^m$ is derived. From the ratio of resonance frequencies in Fe and Ni, it can be stated definitively that the NMR-ON result on $^{110}\text{Ag}^m\text{Ni}$ of Fox *et al.*¹⁰ is not correct. In addition, we compare the recoil-implantation behavior of Ag in Fe with the mass-separator implantation behavior of Ag in Fe studied recently by Nuytten *et al.*¹² The fact that AgFe samples can be well prepared by the recoil-implantation technique is also interesting in context with the study of the relaxation behavior of $3d$, $4d$, and $5d$ impurities in Fe, Co, and Ni, especially the field dependence of the spin-lattice relaxation process.

II. EXPERIMENTAL PROCEDURE

A. Nuclear orientation (NO) and NMR on oriented nuclei (NMR-ON)

The angular distribution of γ rays emitted in the decay of oriented nuclei is given by¹³

1199 keV transition can be calculated unambiguously, as the tensor rank of the (allowed) electron capture (EC) decay to the 2757 keV level is uniquely given by $L_\beta=1$. This means that the γ anisotropy of this transition, together with the NMR-ON value for the hyperfine splitting, will allow the determination of the fraction of Ag nuclei occupying regular lattice sites.

III. EXPERIMENTAL DETAILS

Samples of $^{106}\text{Ag}^m$ in Fe and Ni were prepared with the recoil-implantation technique. A sandwich target consisting of 16 ^{106}Pd foils (isotopic enrichment 98.5%, thickness 1.7 mg/cm²), each followed by a 1.6 mg/cm² Fe (or Ni) foil (purity 99.999%), was irradiated with 68 MeV α particles at the cyclotron in Karlsruhe for 5 h with an average current of 2 μA . As a result of the reaction kinematics, the $^{106}\text{Ag}^m$ nuclei which are produced via the $^{106}\text{Pd}(\alpha,3n\text{p})$ compound reaction (estimated cross section ~ 300 mb) have a kinetic energy of ~ 2.5 MeV. This kinetic energy is sufficiently large that the $^{106}\text{Ag}^m$ nuclei which are produced in the rear ~ 0.2 μm surface layers of the Pd foils leave the target foils. These nuclei are implanted homogeneously into the Fe/Ni catcher foils within a thickness of ~ 0.2 μm . The homogeneous distribution of impurity nuclei in the catcher foils is a decisive advantage in comparison to mass-separator implantation, where the implantation depth is, in general, smaller by a factor of ~ 10 , and, in addition, the implanted nuclei are not distributed homogeneously. After the irradiation eight foils were soldered with GaIn to the copper cold-finger of an adiabatic demagnetization cryostat and cooled to a temperature of ~ 8 mK. The samples were polarized with an external magnetic field $B_0 \leq 4$ kG. The radio frequency field was applied with a one-turn rf coil; it was 1 kHz frequency modulated with a total bandwidth of 0.1–2 MHz. The center frequency was varied in steps

of 0.05–1 MHz over the resonance region. The γ radiation was detected with two 80 cm³ coaxial Ge(Li) detectors placed at 0° and 90° with respect to B_0 . γ -ray spectra were accumulated for 200 s at fixed frequencies. After the accumulation the spectra were recorded onto magnetic tape. The intensities of all γ rays of interest were determined with least-squares fitting routines. Always an even number of single resonance spectra were added which had been measured with increasing and decreasing center frequency in order to avoid possible shifts of the (effective) resonance centers due to the finite spin-lattice relaxation time. In order to investigate the annealing properties of AgFe an independent experiment was performed. After the irradiation, eight foils were annealed for 2 h at $\sim 650^\circ\text{C}$ in a high vacuum atmosphere with pressure $\lesssim 10^{-6}$ Torr. The cooling down to room temperature was performed slowly within ~ 3 h. In this experiment smaller linewidths of the NMR-ON resonances were obtained. The γ anisotropies of 18 transitions were measured in a magnetic field $B_0=3.2$ kG at a temperature $T=10.0(3)$ mK, which was determined from the γ anisotropy of ^{54}Mn , which appeared as a contaminant activity produced by the α irradiation in the Fe foils. Samples of $^{106}\text{Ag}^m\text{Ni}$ were prepared in a similar manner; they were not annealed for the NMR-ON experiments.

IV. RESULTS

A. γ anisotropies

From the γ anisotropies $W(0,T)$ and $W(90,T)$ measured at $T=10.0(3)$ mK for the annealed sources, experimental values for A_2 and A_4 were determined via the linear combinations W_2 and W_4 of Eq. (3), where the $B_{2,4}$ coefficients were calculated with the NMR-ON value for the hyperfine splitting (see Sec. IV B). In this way, independent values for A_2 and A_4 are obtained, which are

TABLE I. Measured $A_{2,4}$ coefficients for transitions in ^{106}Pd .

E (keV)	E_i (keV)	E_f (keV)	I_i^π	I_f^π	A_2	A_4
222	2306	2084	4 ⁻	3 ⁻	+ 0.41(2)	-0.10(4)
391	2757	2366	5 ⁺	5 ⁺	+ 0.24(2)	-0.36(4)
406	2757	2351	5 ⁺	4 ⁺	+ 0.49(2)	+ 0.36(4)
430	1558	1128	3 ⁺	2 ⁺	+ 0.07(1)	+ 0.16(4)
451	2757	2306	5 ⁺	4 ⁻	+ 0.28(1)	-0.05(3)
616	1128	512	2 ⁺	2 ⁺	+ 0.08(1)	-0.03(3)
703	1932	1229	4 ⁺	4 ⁺	+ 0.27(4)	-0.03(8)
717	1229	512	4 ⁺	2 ⁺	-0.31(1)	-0.06(3)
748	2306	1558	4 ⁻	3 ⁺	+ 0.26(1)	-0.07(3)
793	2351	1558	4 ⁺	3 ⁺	+ 0.14(3)	-0.03(6)
804	1932	1128	4 ⁺	2 ⁺	-0.32(2)	-0.06(4)
808 ^a	2366	1558	5 ⁺	3 ⁺	-0.26(3)	+ 0.02(6)
825	2757	1932	5 ⁺	4 ⁺	+ 0.26(2)	+ 0.48(4)
1046	1558	512	3 ⁺	2 ⁺	+ 0.28(1)	+ 0.17(3)
1128	1128	0	2 ⁺	0 ⁺	-0.25(2)	+ 0.07(5)
1199	2757	1558	5 ⁺	3 ⁺	-0.42(2)	-0.17(5)
1223	2351	1128	4 ⁺	2 ⁺	-0.32(3)	-0.14(6)
1528	2757	1229	5 ⁺	4 ⁺	+ 0.65(2)	+ 0.39(4)

^aIncluding a contamination from ^{105}Ag .

listed in Table I. The “full-field” fraction f was found to be 0.88(2).

B. NMR-ON on $^{106}\text{Ag}^m\text{Fe}$

With an external magnetic field $B_0=0.80(2)$ kG, the resonance was searched by varying the center frequency in 1 MHz steps, starting at 190 MHz, and analyzing the intensities of the strongest γ transitions. (Counting time 200 s, modulation width ± 1 MHz.) After the resonance signal was detected at ~ 210 MHz, the frequency region was reduced, and the further measurements were performed with a resolution of 0.2 MHz and a frequency modulation bandwidth of ± 0.3 MHz. Figure 2 shows NMR-ON resonances of the 1528 keV transition measured in external fields of 0.80(2), 2.40(5), and 4.0(1) kG. The total resonance linewidth (including the broadening

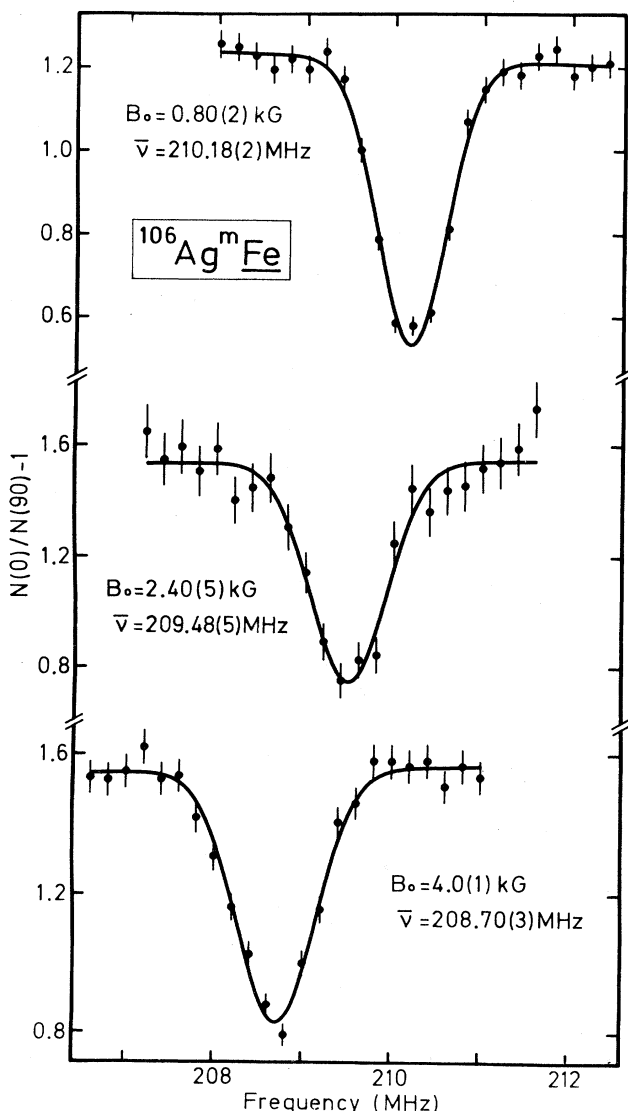


FIG. 2. $^{106}\text{Ag}^m\text{Fe}$ NMR-ON resonances of the 1528 keV transition for the unannealed sample in different external magnetic fields B_0 . The total resonance linewidths (including the broadening due to the frequency modulation bandwidth of ± 0.3 MHz) are ~ 1.0 MHz.

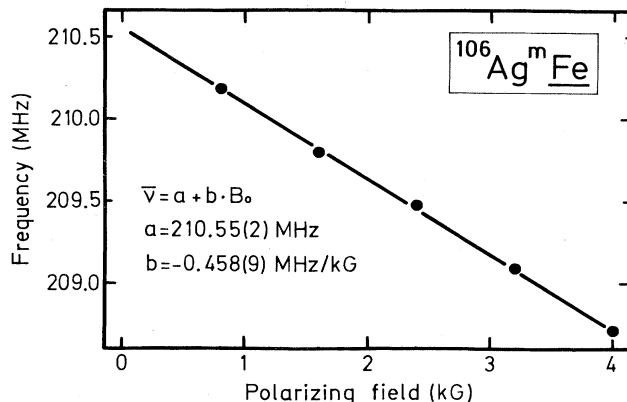


FIG. 3. Shift of the NMR-ON resonances of $^{106}\text{Ag}^m\text{Fe}$ with the external magnetic field B_0 .

due to the frequency modulation bandwidth of ± 0.3 MHz) was found to be ~ 1.0 MHz, which is smaller than the linewidth reported for a mass separator-implanted (not annealed) sample of $^{110}\text{Ag}^m$ in a Fe single crystal.¹⁶ The resonance centers versus polarizing field are shown in Fig. 3. The least squares fit yields

$$\bar{\nu}(B_0=0) = 210.55(2) \text{ MHz},$$

$$d\bar{\nu}/dB_0 = -0.458(9) \text{ MHz/kG}.$$

For the annealed samples, NMR-ON measurements were performed only for $B_0=0.80(2)$ kG, with modulation bandwidths of ± 0.05 , ± 0.1 , and ± 0.2 MHz. A NMR-ON resonance of the 1528 keV transition is shown in Fig. 4. The average center frequencies of the 16 strongest γ transitions were found to be 210.137(3), 210.141(3), and 210.148(2) MHz, respectively. The slightly different effective center frequencies for the measurement with different modulation bandwidths strongly indicate that a small quadrupole splitting is superimposed on the magnetic hyperfine splitting. Therefore, the resonance displacements $(\bar{m} + \frac{1}{2})$ for $\theta=0^\circ$ and 90° , c_0 and c_{90} , were

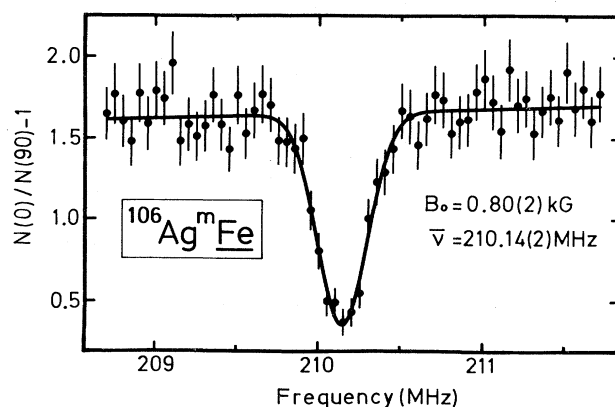


FIG. 4. NMR-ON resonance of the 1528 keV transition of the annealed $^{106}\text{Ag}^m\text{Fe}$ sample measured in an external magnetic field $B_0=0.80(2)$ kG. In comparison to the unannealed sample, the linewidth is considerably smaller, $\Gamma=0.36(2)$ MHz (including the broadening due to the frequency modulation bandwidth of ± 0.1 MHz). In comparison to the unannealed sample the resonance amplitude is larger by a factor of ~ 2 .

calculated as outlined in detail in Ref. 15. In Table II c_0 and c_{90} are listed, which were calculated with the following parameters: $T=10$ mK; ratio of total modulation linewidth to quadrupole subresonance separation equals 6, stepwidth to quadrupole subresonance separation equals 3, measurement time per step 200 s. The Korringa constant for AgFe was taken from Ref. 11. The quadrupole splitting was determined by a self-consistent iteration procedure. The result is

$$\Delta\nu_Q = +0.012(6) \text{ MHz},$$

$$\nu_Q = +0.53(27) \text{ MHz},$$

which means that a correction of 0.03(2) MHz has to be applied to the effective zero-field hyperfine splitting frequency to obtain the pure magnetic hyperfine splitting. The average effective resonance center of the 0.80(2) kG spectra of the unannealed sample is 210.182(5) MHz. The difference of ~ 0.04 MHz to the annealed samples cannot be ascribed completely to quadrupole effects. This shows that the average hyperfine splitting deduced from the center of the resonance lines depends (in this case slightly) on the treatment of the samples. It is astonishing that a larger hyperfine splitting is deduced from the sample with the larger linewidth, which indicates that the hyperfine splitting is not necessarily reduced by crystal imperfections, but may be enhanced. Taking into account the displacement due to the quadrupole interaction and the uncertainty due to the differences of the effective center frequencies, the magnetic hyperfine splitting of $^{106}\text{Ag}^m$ in Fe is finally deduced to be

$$\nu_M(^{106}\text{Ag}^m\text{Fe}) = 210.57(3) \text{ MHz}.$$

It should be noted that the linewidth of ~ 0.3 MHz obtained in the measurement with a modulation bandwidth of ± 0.05 MHz is rather small. It has to be compared

TABLE II. Calculated resonance displacements of different transitions for $\theta=0^\circ$ and 90° at $T=10$ mK in units of the quadrupole subresonance separation $\Delta\nu_Q$. (Modulation width equals $6|\Delta\nu_Q|$.)

E/keV	c_0	c_{90}
222	-3.21	-3.53
391	(+ 1.00)	-3.92
406	-3.79	-2.86
430	-4.16	(+ 5.70)
451	-3.27	-3.50
616	-3.08	-3.58
703	-3.32	-3.46
717	-3.53	-3.30
748	-3.19	-3.54
793	-3.24	-3.51
804	-3.53	-3.30
808	-3.35	-3.45
825	-4.09	(-0.13)
1046	-3.74	-2.99
1128	-3.18	-3.54
1199	-3.65	-3.15
1223	-3.66	-3.13
1528	-3.73	-2.99

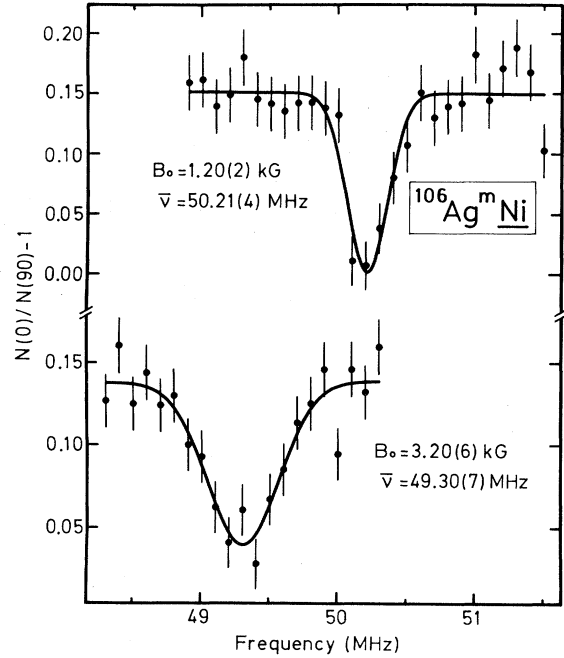


FIG. 5. $^{106}\text{Ag}^m\text{Ni}$ NMR-ON resonances of the 1528 keV transition for different external magnetic fields B_0 .

with $\Gamma=0.65(5)$ MHz obtained by Duczynski¹⁶ with $^{110}\text{Ag}^m$ in an Fe single crystal prepared by mass-separator implantation and subsequent annealing.

C. NMR-ON on $^{106}\text{Ag}^m\text{Ni}$

With Ni as host lattice, NMR-ON measurements were performed on unannealed samples. Two NMR-ON spectra of the 1528 keV transition measured in external magnetic fields of 1.20(2) and 3.20(6) kG are shown in Fig. 5. Additional measurements were performed for $B_0=2.20(4)$ kG. The linewidths were found to be 0.33(7), 0.51(8), and 0.59(8) MHz for the measurements with $B_0=1.20, 2.20,$ and 3.20 kG, respectively. The increasing linewidth is probably due to experimental reasons: It is known that the spin-lattice relaxation time for Ag in Ni is considerably longer than the spin-lattice relaxation time in Fe, and that a field dependence exists, corresponding to larger relaxation times with increasing polarizing field.¹¹ As our measurements were performed with a constant "sweep" rate for the center frequency of 0.3 kHz/s, the centers of single NMR-ON spectra are shifted in sweep direction. In order to compensate the influence of this effect on the resonance center, always an even number of NMR-ON spectra with opposite sweep direction were added. The observed linewidth is artificially broadened by this procedure, but the resonance centers are unaffected, as has been shown in Ref. 17. The resonance centers versus B_0 are illustrated in Fig. 6. From a least squares fit

$$\bar{\nu}(B_0=0) = 50.76(4) \text{ MHz},$$

$$d\bar{\nu}/dB_0 = -0.456(16) \text{ MHz/kG},$$

is obtained. No resonance displacement of the NMR-ON

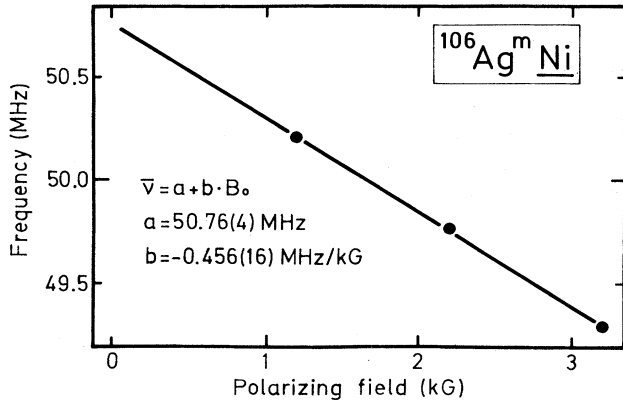


FIG. 6. Shift of the NMR-ON resonances of $^{106}\text{Ag}^m\text{Ni}$ with the external magnetic field B_0 .

resonances of different transitions could be detected, first, because of the small γ anisotropies due to the smaller hyperfine splitting (the ratio $h\nu_M/k_B T$ is only ~ 0.2 at $T = 10$ mK), and second, because the quadrupole splitting is expected to be smaller than that in Fe. No further attempts were made to perform measurements on annealed samples as the accuracy obtained in this experiment was sufficient to derive a reliable value for the hyperfine field of Ag in Ni.

V. DISCUSSION

A. Hyperfine interaction aspects

The currently known magnetic hyperfine splitting frequencies of Ag isotopes in Fe and Ni are listed in Table III. Our ratio for the hyperfine splittings of $^{106}\text{Ag}^m$ in Fe and Ni, 4.148(5), is in perfect agreement with the corresponding ratio for $^{110}\text{Ag}^m$ of Rüter *et al.*,¹¹ 4.145(5), and proves uniquely that the NMR-ON frequency of $^{110}\text{Ag}^m\text{Ni}$ and thus the value for the hyperfine field of AgNi of Fox *et al.*¹⁰ is incorrect. Taking the magnetic moment of $^{110}\text{Ag}^m$ as $\mu = 3.607(4) \mu_N$,^{2,3} the g factor and magnetic moment of $^{106}\text{Ag}^m$ are from the ratio of resonance frequencies found to be

$$g(^{106}\text{Ag}^m) = (+)0.6182(7),$$

$$\mu(^{106}\text{Ag}^m) = (+)3.709(4) \mu_N.$$

Here hyperfine anomalies can be neglected, as the structure of both states is similar and the magnetic moments are nearly equal. The hyperfine fields of Ag in Fe and Ni are the following:

$$B_{\text{HF}}(\text{AgFe}) = -446.9(5) \text{ kG},$$

$$B_{\text{HF}}(\text{AgNi}) = -107.7(2) \text{ kG}.$$

With the known NMR-ON frequency the γ anisotropies of $^{106}\text{Ag}^m\text{Fe}$ of the unannealed and annealed sample can be interpreted. In the framework of a two-site model we find the fraction of Ag nuclei on full-field lattice sites to be $f \geq 0.90$ and $0.88(2)$ for the unannealed and annealed sample, respectively. (The uncertainty for the unannealed sample is due to the fact that the temperature was determined from the γ anisotropy of ^{54}Mn , which appeared as contaminant activity, for which the fraction f is also unknown. It has been estimated from the systematics on other recoil-implantation experiments, in which a second independent thermometer had been used.) This can be compared with the result of Duczynski,¹⁶ who obtained $f = 1.0, 1.0,$ and 0.80 for (room-temperature) mass-separator implantation into polycrystalline Fe foils, a $\langle 001 \rangle$ Fe single crystal, and a $\langle 110 \rangle$ Fe single crystal, respectively. Nuytten *et al.*¹² studied the implantation behavior of In and Ag in Fe at low temperatures. They argued that the chance for implanted impurities of populating the substitutional site might increase for low-temperature implantations compared to room-temperature implantations or implantation at higher doses. These conclusions were drawn from the fact that Cohen *et al.*¹⁸ obtained only a fraction of $0.44(3)$ in a room temperature implantation of $^{110}\text{Ag}^m$ into Fe. The results on the room temperature implantation of $^{110}\text{Ag}^m$ into Fe of Duczynski¹⁶ mentioned before contradict this speculation. It should be noted, however, that the narrowest NMR-ON resonance lines were obtained with the (room-temperature) recoil-implanted $^{106}\text{Ag}^m\text{Fe}$ samples of the present work, which proves that the crystal structure is less destroyed in this type of implantation. Moreover, the samples prepared by recoil implantation can be annealed without losing a significant fraction of nuclei on full-field lattice sites. (Duczynski¹⁶ reported a significant reduction of f from ~ 0.80 to ~ 0.50 after annealing a $\langle 110 \rangle$ $^{110}\text{Ag}^m\text{Fe}$ single crystal sample.) Here it should be added that the resonance amplitude with the annealed $^{106}\text{Ag}^m\text{Fe}$ sample was larger by a factor of ~ 2 than the corresponding resonance amplitude of the unannealed sample, although the full-field fractions were almost identical.

From the resonance shifts with the external magnetic field B_0 $|g(1+K)|$ is deduced to be $0.601(12)$ and $0.598(21)$ for Fe and Ni as host lattice, respectively. With the g factor known more precisely from the zero-field splitting, the Knight shift parameters are deduced to be $K_{\text{Fe}} = -0.03(2)$ and $K_{\text{Ni}} = -0.03(4)$, which agree within

TABLE III. Hyperfine splittings of Ag isotopes in Fe and Ni.

Isotope	I^n	$\bar{\nu}_{\text{Fe}}/\text{MHz}$	$\bar{\nu}_{\text{Ni}}/\text{MHz}$	$\bar{\nu}_{\text{Fe}}/\bar{\nu}_{\text{Ni}}$	Ref.
$^{106}\text{Ag}^m$	6^+	210.57(3)	50.76(4)	4.148(5)	This work
$^{110}\text{Ag}^m$	6^+	204.8(2)	56.0(2)	3.66(2)	10
		204.78(2)	49.40(4)	4.145(5)	11

TABLE IV. Multipole mixing ratios.

E/keV	$\mathcal{M}L'/\mathcal{M}L$	δ
222	$E2/M1$	-0.08(2)
391	$M1/E2$	-0.03(8)
		-0.6(2)
406	$E2/M1$	-3.5(2)
430	$E2/M1$	-9(1)
616	$M1/E2$	-0.07(4)
		-1.9(2)
703	$M1/E2$	-0.6(4)
793	$E2/M1$	+0.06(3)
		-8(2)
825	$E2/M1$	-6.8(6)
1046	$E2/M1$	-3.8(3)
1528	$E2/M1$	-2.5(1)

one standard deviation with $K_{\text{Fe}} = -0.047(5)$ and $K_{\text{Ni}} = +0.007(7)$, which were deduced by Duczynski¹⁶ from the resonance shifts of $^{110}\text{Ag}^m$.

B. Levels and multipole mixing ratios of ^{106}Pd

With the experimental $A_{2,4}$ coefficients listed in Table I, multipole mixing ratios δ were determined with a *simultaneous* least-squares fit of all $A_{2,4}$ coefficients to the complex decay scheme. A simultaneous fit is necessary as the δ 's influence not only the γ anisotropy of the respective observed transition but also the orientation of the levels following in the decay cascade via the deorientation coefficients U_k (and thus the γ anisotropies of all transitions in the cascade). The results are listed in Table IV. For the 391, 616, and 793 keV transitions the accuracy of A_4 did not allow to exclude definitely one of the two results for δ obtained from the more sensitive A_2 . Therefore both results are listed in Table IV. In Table V we have compiled the $E2$ fractions $\delta^2/(1+\delta^2)$, together with the respective results of Schoeters *et al.*,⁵ Grau *et al.*,¹⁹

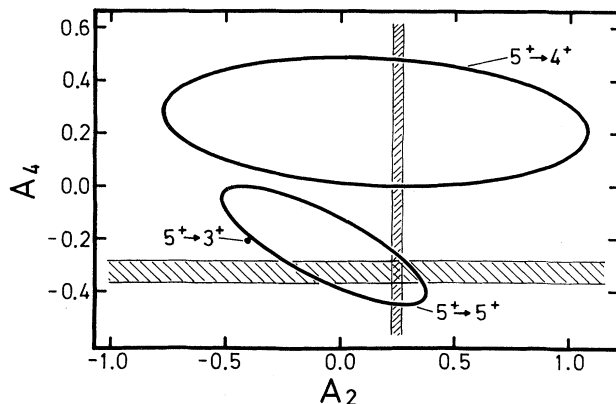


FIG. 7. A_2 - A_4 plot for the 391 keV transition with the assumption of $I^\pi = 3^+, 4^+$, or 5^+ for the 2366 keV level in ^{106}Pd . The experimental $A_{2,4}$ data definitely rule out $I^\pi = 4^+$, which was adopted before.

Tivin *et al.*,²⁰ Shevelev *et al.*,²¹ and Babenko *et al.*²² With the exception of the 793 keV transition, most ambiguities are removed now.

However, our data are inconsistent with an assignment $I^\pi = 4^+$ for the 2366 keV level assumed previously.⁵ Originally $I = 3, 4$ had been assumed for this level. It is fed in the cascade

$$5^+(2757) \xrightarrow{391} 3^+, 4^+, 5^+(2366) \xrightarrow{808} 3^+(1558),$$

where we added the possibility $I = 5$. The assignment of the correct spin can thus be performed via the $A_{2,4}$ coefficients of the 391 and the 808 keV transitions. Figure 7 shows the allowed $A_{2,4}$ combinations for the 391 keV transition for $I^\pi = 3^+$ ($E2$), $I^\pi = 4^+$ ($E2+M1$), and $I^\pi = 5^+$ ($E2+M1$). It is obvious that $I^\pi = 3^+$ can be excluded from A_2 . To exclude either 4^+ or 5^+ , the independent knowledge of A_2 and A_4 is necessary. Schoeters *et al.*⁵ analyzed $\epsilon(T)$, which is not sensitive to

TABLE V. $E2$ fractions $\delta^2/(1+\delta^2)$ for mixed $E2/M1$ transitions.

E (keV)	This work	Ref. 5	Ref. 20	Ref. 21	Ref. 22
222	0.006(4)	0.017(5)	0.006(\pm^{19})	0.030(7)	
391	0.999(\pm^{11}) 0.77(10)	0.996(\pm^4)		0.80 (25)	
406	0.925(13)	0.91(1)	0.98(\pm^1)	1.0-0.15	
430	0.988(3)	0.982(3)	0.9-0.999	0.30(12)	dominant $E2$
616	0.995 \pm^4 0.22(4)	0.990(5)	0.989(\pm^4)	1.0-0.13	dominant $E2$
703	0.73(24)	0.54(14)	0.84(\pm^2) 1.00-0.96	0.16(10)	
793	0.985(12) 0.004(4)	0.980(\pm^5) 0.00(1)	0.95(\pm^6) 0.14(9)	1.0-0.12	dominant $E2$
825	0.979(4)	0.97(1) 0.002(2)		0.68(14)	
1046	0.935(11)		0.96(\pm^1) 0.14(3)	0.20-0.08	dominant $E2$
1528	0.864(12)	0.84(2) 0.07(1)	0.85(\pm^6) 0.23(10)		

the difference between 4^+ and 5^+ . From the independent determination of A_2 and A_4 via $W_2(T)$ and $W_4(T)$, $I^\pi=4^+$ must be excluded. Thus $I^\pi=5^+$ is proposed for the 2366 keV level. The $A_{2,4}$ data for the 808 keV transition, which deexcites the 2366 keV level, are consistent with a pure $E2$ multipolarity. In this context we want to point out that the mixing ratios deduced from the present work are partly in disagreement with the recommended values in the table of Krane.²³ Furthermore, our $A_{2,4}$ data are partly in disagreement with $A_{2,4}$ data of Grau *et al.*¹⁹

C. Magnetic moment

The magnetic moment of $^{106}\text{Ag}^m$, $|\mu| = 3.709(4) \mu_N$, is in good agreement with the less precise value $|\mu| = 3.71(15) \mu_N$, derived by Haroutunian *et al.*⁶ from a simultaneous measurement of $^{106}\text{Ag}^m$ and $^{110}\text{Ag}^m$. This proves that the NO measurement of Schoeters *et al.*⁵ must have been misinterpreted, from which $\mu = 2.8(2) \mu_N$ had been deduced. The argument of Haroutunian *et al.*⁶ that "the $E2/M1$ mixing ratios given in Ref. 5 are not affected within experimental errors by the erroneous magnetic moment used, as the distribution parameters were normalized to a pure $E2$ transition," is not correct. In Sec. V A it has been shown that the multipole mixing ratios deduced in this work are partly different from those of Ref. 5. This proves again the necessity of applying independent techniques, such as NO and NMR-ON in the present case, for the determination of the magnetic moment and the decay parameters.

The magnetic moments of $^{106,108,110}\text{Ag}$ and

TABLE VI. Magnetic moments of $^{106,108,110}\text{Ag}$ and $^{106,108,110}\text{Ag}^m$.

Isotope	I^π	μ/μ_N	Ref.
^{106}Ag	1^+	2.85(20)	24
^{108}Ag	1^+	2.6884(7)	25
^{110}Ag	1^+	2.7271(8)	25
$^{106}\text{Ag}^m$	6^+	3.709(4)	This work
$^{108}\text{Ag}^m$	6^+	3.580(20)	2
$^{110}\text{Ag}^m$	6^+	3.607(4)	2

$^{106,108,110}\text{Ag}^m$ are listed in Table VI. The 1^+ ground states and the 6^+ isomers are described by the antiparallel and parallel coupling of $(\pi g_{9/2})_{7/2^+}^{-3}$ and $(\nu d_{5/2})_{5/2^+}^{-1}$ shell model states. The small variation of the magnetic moments of the ground states and the isomers suggest that the neutron core polarization influences the magnetic moments of these states only weakly.

ACKNOWLEDGMENTS

We are indebted to Prof. P. Kienle for his kind interest and continuous support of this work. We also wish to thank K. Assmus and the Karlsruhe cyclotron crew for performing the alpha irradiations and E. Smolic and J. Hesol for experimental help. This work was supported by the Bundesministerium für Forschung und Technologie, Bonn, Federal Republic of Germany, and, partly, by the Kernforschungszentrum, Karlsruhe, and the Walther Meissner Institut für Tieftemperaturforschung, Garching, Federal Republic of Germany.

¹Table of Isotopes, edited by C. M. Lederer and V. S. Shirley, 7th ed. (Wiley, New York, 1978), Appendix VII, p. A-42.

²W. Fischer, H. Hühnermann, and Th. Meier, Z. Phys. A **274**, 79 (1975).

³F. D. Feiock and W. R. Johnson, Phys. Rev. **187**, 39 (1969).

⁴W. Easley, N. Edelstein, M. P. Klein, D. A. Shirley, and H. H. Wickmann, Phys. Rev. **141**, 1132 (1966).

⁵E. Schoeters, R. Geerts, R. E. Silverans, and L. Vanneste, Phys. Rev. C **12**, 1680 (1975).

⁶R. Haroutunian, G. Marest, and I. Berkes, Phys. Rev. C **14**, 2016 (1976).

⁷K. S. Krane, Hyperfine Interact. **15/16**, 1069 (1983).

⁸M. Hansen, Constitution of Binary Alloys, 2nd ed. (McGraw-Hill, New York, 1958).

⁹E. Matthias and R. J. Holliday, Phys. Rev. Lett. **17**, 897 (1966).

¹⁰R. A. Fox, P. D. Johnston, and N. J. Stone, Phys. Lett. **34A**, 211 (1971).

¹¹H. D. Rüter, E. W. Duczynski, G. Scholtyssek, S. Kampf, E. Gerdau, and K. Freitag, Proceedings of the Sixth International Conference on Hyperfine Interactions, Groningen, The Netherlands, 1983, Book of Abstracts, p. RP 8.

¹²C. Nuytten, D. Vandeplassche, E. van Walle, and L. Vanneste, Phys. Lett. **92A**, 139 (1982).

¹³S. R. de Groot, H. A. Tolhoek, and W. J. Huiskamp, in Alpha,

Beta, and Gamma Ray Spectroscopy, edited by K. Siegbahn (North-Holland, Amsterdam, 1968), Vol. 2, p. 1199.

¹⁴T. Yamazaki, Nucl. Data Sect. A **3**, 1 (1967).

¹⁵E. Hagn, Phys. Rev. B **25**, 1521 (1982).

¹⁶E. Duczynski, Ph.D. thesis, Universität Hamburg, 1983 (unpublished).

¹⁷E. Hagn, E. Zech, and G. Eska, Phys. Rev. C **23**, 2252 (1981).

¹⁸E. J. Cohen, H. R. Andrews, T. F. Knott, F. M. Pipkin, and D. C. Santry, Phys. Rev. C **20**, 847 (1979).

¹⁹J. A. Grau, L. E. Samuelson, F. A. Rickey, P. C. Simms, and G. J. Smith, Phys. Rev. C **14**, 2297 (1976).

²⁰P. J. Tivin, B. Singh, and H. W. Taylor, J. Phys. G **3**, 1267 (1977).

²¹G. A. Shevelev, A. G. Troitskaya, and V. M. Kartashov, Bull. Acad. Sci. USSR, Phys. Ser. **42**, No. 12, 128 (1978).

²²V. V. Babenko, I. N. Vishnevskii, V. A. Zheltonozhskii, V. P. Svyato, A. G. Sergeev, and V. V. Trishin, Bull. Acad. Sci. USSR, Phys. Ser. **43**, No. 5, 20 (1979).

²³K. S. Krane, At. Data Nucl. Data Tables **20**, 211 (1977).

²⁴B. Greenebaum and E. A. Phillips, Phys. Rev. C **9**, 2028 (1974).

²⁵A. Winnacker, H. Ackermann, D. Dubbers, M. Grupp, P. Heitjans, and H.-J. Stöckmann, Nucl. Phys. A **261**, 261 (1976).